Optical Materials 92 (2019) 366–372

Contents lists available at ScienceDirect

Optical Materials

journal homepage: www.elsevier.com/locate/optmat

Comparative analyses of optical limiting effects in metal nanoparticles and perovskite nanocrystals

Konda Srinivasa Rao[a], Rashid A. Ganeev[a], Ke Zhang[a], Yue Fu[a], Ganjaboy S. Boltaev[a], Sandeep Kumar Maurya[a], Chunlei Guo[a,b,*]

[a] The Guo China-US Photonics Laboratory, State Key Laboratory of Applied Optics, Changchun Institute of Optics, Fine Mechanics and Physics, Chinese Academy of Sciences, Changchun, 130033, China
[b] The Institute of Optics, University of Rochester, Rochester, NY, 14627, USA

ARTICLE INFO

Keywords:
Optical limiting
Nanoparticles
Perovskites
Quantum dots
Nonlinear absorption
Nanocrystals

ABSTRACT

This paper reports the comprehensive comparative study of absorptive nonlinear optical limiting among metal nanoparticles, quantum dots, and perovskites using 60 fs, 800 nm laser pulses. The metal nanoparticles include Al, Ti, Co, Ni, Zn, Ag, Sn, In, W, Au and the quantum dots of Ag_2S, and finally the perovskites such as $CsPbBr_3$ and $CsPbI_2Br$. We systematically characterized all materials mentioned above using absorption spectra and scanning electron microscope. We demonstrate that the light-induced nonlinear absorption leads to optical limiting. The suspensions of the reported samples demonstrated low threshold of optical limiting, which can be explained by strong two-photon absorption in these solutions. The gold nanoparticles (10–30 nm) show the lowest threshold of optical limiting (3.26 mJ cm^{-2}).

1. Introduction

The study of optical limiting with metallic nanoparticles has attracted a tremendous amount of attention of due to its increased demand for protection against laser threats to sensors and human eyes. One major approach is the utilization of nanoparticles as optical limiters. Metal nanoparticles (NPs) and quantum dots (QDs) have attracted much attention due to their high surface-to-volume ratio and quantum confinements [1]. These nanocomposites have special nonlinear optical behavior as compared to the bulk materials. For instance, optical nonlinearities and optical limiting (OL) effects of the nanocomposites of the metals can be significantly enhanced by increasing the number density and low dimensionality of the metal particles [2]. NPs display a drastic optical extinction due to their nonlinear scattering. Among metal nanoparticle limiters, gold and silver NPs [1–5] have received special attention since they both exhibit a broad surface plasmon resonance (SPR) absorption band in the visible region, which is substantially different from the flat absorption of the corresponding bulk metals in this region. Nanostructured nonlinear optical materials have been used as submissive and operative optical limiters to reduce the optical transmittance of the incident laser radiation by virtue of their intrinsic optical properties [6–13].

The optical limiting is one of the potential applications of the materials' optical nonlinearities. It is mainly aimed at protecting eyes and sensitive registration devices from damaging. The aim of this paper was to present the comparative analysis of the optical limiting effect based on the nonlinear optical characteristics of materials. For preparation of the liquid solution of NPs, we used a laser ablation technique. Among the benefits of laser ablation is that it can be performed using both a pulsed wave and continuous wave lasers, although the former method is dominant due to higher peak intensities of pulsed lasers. This technique allows synthesizing pure NPs in colloidal form depending on the purity of target used for laser ablation, compared to chemical methods. Pulsed laser ablation in the liquid environment provides a green, safe and efficient synthesis compared to chemical reduction method. Moreover, it can be used to synthesize the NPs from the metals with different hardness and melting point [14]. In case of Ag NPs, we compared the optical limiting of monodispersed silver NPs suspensions prepared by chemical reduction and laser ablation techniques [15]. In both cases, the shape of absorption curves and peak position of surface plasmon resonances (SPR) were similar to each other. Tutt et al. studied the optical limiting effect of low dimensional species [16]. They demonstrated the advantages of the low dimensional carbon nanostructures in the determination of optical limiting. In our present study, we analyzed

* Corresponding author. The Guo China-US Photonics Laboratory, State Key Laboratory of Applied Optics, Changchun Institute of Optics, Fine Mechanics and Physics, Chinese Academy of Sciences, Changchun, 130033, China.
E-mail addresses: guo@ciomp.ac.cn, guo@optics.rochester.edu (C. Guo).

https://doi.org/10.1016/j.optmat.2019.04.058
Received 25 February 2019; Received in revised form 22 April 2019; Accepted 26 April 2019
Available online 06 May 2019
0925-3467/ Published by Elsevier B.V.

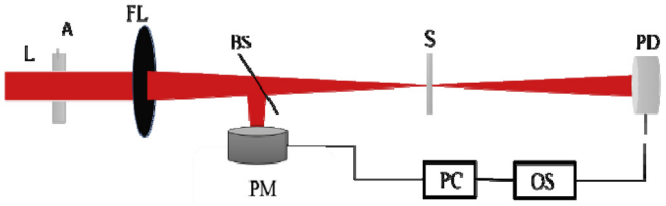

Fig. 1. Experiment layout for optical limiting studies. L: laser, 800 nm, 60 fs, 1 kHz, A: attenuator, FL: focal lens, f = 400 mm, S: sample, BS: beam splitter, PM: power meter, PD: photodiode, PC: personal computer, OS: oscilloscope.

the optical limiting of NPs suspensions at various sizes, and quantum dots, perovskite nanocrystals using 800 nm laser pulses of duration 60 fs. Additionally, we demonstrated the advantages of gold NPs as the optical limiter at 800 nm pulses of duration 60 fs.

The study of OL of laser radiation in various metallic NPs, QDs, and perovskites opens the possibility of these materials as optical laser shutters to protect against intense laser irradiation and to investigate the fundamental properties of nonlinear optical media [17–21]. The OL mechanisms have different origins. In molecules, the OL mechanism is governed by reverse saturable absorption (RSA) due to the large cross-section of excited state absorption. It was observed that two-photon absorption (2 PA) might responsible for OL in our present study of Al, Ti, Co, Ni, Zn, Ag, Sn, In, W, Au NPs, Ag_2S quantum dots, and $CsPbBr_3$, $CsPbI_2Br$ perovskites.

2. Experimental arrangement

The experimental arrangement for OL is shown in Fig. 1. The sample (colloidal solutions put in 2 mm cuvette) has been scanned along the focal plane of laser pulses. At the focal point, the sample experiences maximal pump intensity, which gradually decreases above and beyond the focus. A lens with focal length of 400 mm is used in the present studies. The OL properties of the mentioned sample suspensions were characterized by fluence-dependent transmittance measurements using 800 nm laser pulses of duration 60 fs and at a repetition rate 1 kHz deliver from a Ti: sapphire laser (Spitfire Ace, Spectra-Physics) head. The measured dimensions of beam waist at focus was ~38 μm and the corresponding peak intensities were $\sim 10^{11}$ W cm^{-2}.

The reported NPs suspensions were prepared by chemical reduction and laser ablation methods using different pulse durations and wavelengths. In brief, Ag and Au NPs as well as Ag_2S QDs (0.375 mg/ml), $CsPbBr_3$ and $CsPbI_2Br$ perovskites are prepared by chemical reduction method. The Al and Ag NPs are prepared by ablation bulk target using nanoseconds (ns) pulses of wavelength 1064 nm, pulse duration 6 ns, at pulse energy 2 mJ and 5 mJ, respectively [15]. Ni, Ti, Co, Zn, Sn, In, and W NPs were produced during the laser ablation of bulk targets using 800 nm, 200 ps pulses at pulse energy 550 μJ [14]. The average time of irradiation was ~30 min in deionized water. Once the colloidal solution of NPs prepared, the characterizations such as UV visible absorption spectroscopy (spectrophotometer, Agilent Technologies) and scanning electron microscopy (SEM) (S-4800, Hitachi) were performed to obtain their surface plasmon resonance (SPR) bands and morphological measurements, respectively. The shape of all the prepared NPs suspensions is in spherical, except In, which has a cubic shape.

3. Results and discussions

There are two major nonlinear absorption mechanisms employed for OL namely RSA and 2 PA. The OL that is determined by 2 PA has many advantages such as (i) negligible linear absorption loss for weak signal, (ii) extremely fast temporal response, and (iii) retaining high beam quality of the transmitted signal. Due to these reasons, 2 PA based devices are suitable not only for OL but also for other applications such as power stabilization, pulse reshaping, spatial field reshaping, etc. [22,23]. In our investigation of OL exhibited by the NPs and perovskites was mostly attributed to the 2 PA at the wavelength of 800 nm. For some of the NPs at lower and, higher input energies possess the saturable absorption (SA) and RSA nonlinear processes. RSA generally arises in a molecular system when the excited state absorption cross section is larger than the ground state cross section [24,25]. The process can be understood by considering a system that is modeled using three vibronically broadened energy levels. The energy level diagram for the electron dynamics in Ag nanoparticles leading to SA and RSA was reported in Ref. [26].

In this paper, we have demonstrated the optical limiting effect of various transition (Au, Ag, Ti, Co, Ni, W, Zn) and post-transition (Al, Sn, and In) metal NPs. Metallic NPs with sizes smaller than the wavelength of light show strong dipolar excitations which in turn exhibit strongly localized surface plasmon resonances (LSPR). LSPRs are the non-propagating excitations of the conduction electrons of metallic NPs coupled to the electromagnetic field. The resonance condition is established when the frequency of light matches the natural frequency of conduction electrons. The surface plasmon resonance is a result of the interaction between the incident light and surface electrons in a conduction band. This interaction produces coherent localized plasmon oscillations with a resonant frequency that strongly depend on the composition, size, geometry, dielectric environment and particle-particle separation distance of NPs. Au and Ag NPs possess strong plasmonic resonances in the visible region of the electromagnetic spectrum. The other metal NPs, such as Ti, Co, Ni, W, Zn, Sn and In NPs, possess LSPR in UV region. The UV-visible absorption spectra are shown in the following sections.

3.1. Characterization and optical limiting properties of noble metal non-reactive nanoparticles

In this section, absorption spectra, SEM images and the results of OL properties of noble metal non-reactive NPs such as Al, Ag, Au NPs, Ag_2S QDs and W, Sn, Zn, and In NPs suspensions are presented. The optical, nonlinear optical and OL properties of the above mentioned NPs suspensions strongly depend on their morphology. Earlier optical limiting studies on Au and Ag NPs are reported in Refs. [27,28]. Fig. 2(a–d) shows the SEM images and size distribution of Ag, Al, and Au NPs, whereas Fig. 2(e) depicts the TEM image of Ag_2S QDs. Fig. 2(g) shows the absorption spectra for these NPs suspensions. The optical properties of Ag: chemical, Ag: ablation, Au NPs and Ag_2S QDs characteristic absorption dominated by SPR peaks 400, 402, 527, and 403 for particle sizes of 13, 8, 17, and 4 nm respectively [Fig. 2(g)]. In case of Ag NPs, the width and position of SPR were varied as a function of particle size and shape. As it was pointed out in many studies, the UV absorption spectra of Ag and Au NPs can be significantly controlled by the parameters of nanoparticle preparation methods. Al NPs shows the absorption SPR bands near to UV region. Fig. 2(h) shows the results of OL properties of Al, Ag, Au NPs, and Ag_2S QDs. When the incident energy of 800 nm pulses was increased above the limiting threshold, the transmitted energy approach a steady value. In addition, we have measured the ratio of linear transmittance with respect to water to the NPs transmittance (nonlinear attenuation factor (N_{af})) before the limiting threshold. OL thresholds (OL_T), N_{af}, size distribution, mean size of reported NPs suspensions and the corresponding nonlinear processes are mentioned in Table 1. Ag NPs prepared by ablation has a particle size distribution i.e. 5–90 nm, range and contains a number of smallest nanoparticles of mean size 8 nm. Whereas, Ag NPs prepared by chemical reduction have size distribution 8–18 nm, at a mean size 13 nm. It was observed that Ag NPs prepared by ablation possesses higher optical limitation compared to the chemically synthesized NPs which could be due to the presence of smallest NPs (~8 nm) in the colloidal solution of Ag NPs by laser ablation., Corresponding TEM analysis is shown in Fig. 2(f). Gold nanoparticles possess high OL properties as compared to Ag NPs, whereas Al NPs show high OL compared to the Ag NPs. This

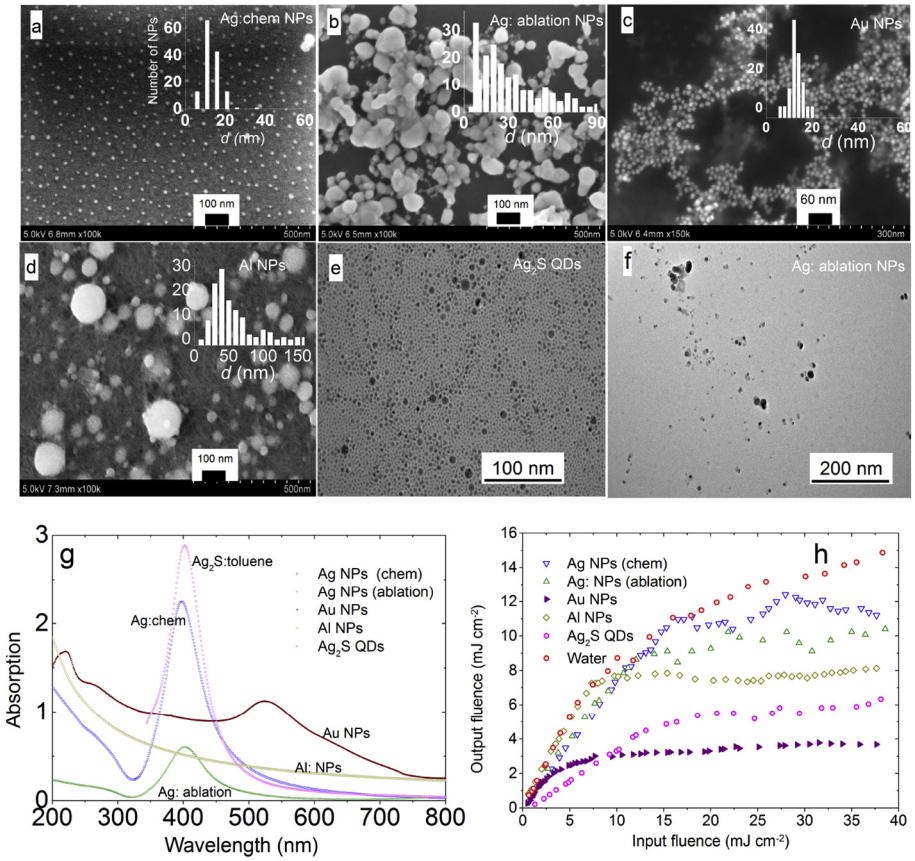

Fig. 2. SEM images and size distribution (x-axis: diameter (*d*) of NPs, Y-axis: Number of NPs) of (a) Ag; chem NPs, (b) Ag: ablation NPs, (c) Au NPs, (d) Al NPs. TEM image of (e) Ag_2S QDs, and (f) Ag: ablation NPs, (g) UV absorption spectra, and (h) optical limiting of Ag, Au and Al NPs suspensions in water and Ag_2S QDs.

Table 1
OL thresholds, nonlinear attenuation factors (N_{af}) and responsible nonlinear optical processes.

NPs	NPs SD (nm)	Mean (nm)	OL_T (mJ cm^{-2})	N_{af}	NP
Nonmagnetic NPs					
Ag: chemical	8–18	13	16.5	1.09	2 PA + SA
Ag: ablation	5–90	8	12.1	1.17	2 PA
Au: chemical	10–30	17	3.26	1.39	2 PA
Al: ablation	10–150	35	7.33	0.87	2 PA
W	4–22	8	13.4	1.75	2 PA
Sn	3–12	7	12.4	2.07	2 PA
Zn	5–30	20	18.8	1.36	2 PA + SA
In	20–120	50	16.8	1.74	2 PA + SA
Magnetic NPs					
Ni	15–250	96	10	1.35	2 PA
Ti	25–250	125	7.6	1.07	SA
Co	5–200	90	8	1.99	2 PA
QDs and perovskites					
Ag_2S QDs	3–6	4	10.2		2 PA
$CsPbBr_3$			6.2		2 PA + SA
$CsPbI_2Br$			13.2		2 PA

might be due to the concentration of Al NPs is larger than the Ag NPs. However, the N_{af} of Al NPs is lower than the N_{af} of Ag NPs. Among Ag NPs, ablated NPs have the highest value of N_{af} (1.17) compared to chemically prepare one (1.09).

From Fig. 2(h), it is observed that the OL curve for Ag_2S, Al NPs, Ag NPs (ablation) shows similar trends. However, Ag NPs (chemical) show a similar trend to Ag NPs (ablation) up to 12.6 mJ cm^{-2}, after this value the output fluence increases. This is probably due to the influence of the size of NPs which is smaller for the case of Ag NPs prepared from ablation method. Among the Ag NPs (prepared by chemical, ablation) and Ag_2S QDs, even though these colloids have nearly equal SPR peaks (Fig. 2(g)), Ag_2S QDs shows higher OL efficiency increased as compared to Ag NPs, due to small size distribution of Ag_2S QDs [Fig. 2(e)]. Other reason for the change in the OL profile in the process of saturable absorption at fluence higher than 23 mJ cm^{-2}. This is in good agreement with the reported value [26,29]. The OL efficiency is increased with small sized NPs like Ag_2S QDs. Au NPs having size distribution range 10–20 nm, mean at 17 nm possess smaller OL threshold (3.26 mJ cm^{-2}) compared to other metal NPs. Also, it might be due to excitation wavelength was closer to the Au SPR wavelength as compared SPR bands of other NPs. The linear dependence input and output pulses were sustained up to the OL threshold of the fluence of the propagated laser radiation. The OL threshold for these NPs is comprised in Table 1. The absence of SPR in Al NPs suspensions as shown in Fig. 2(g) results in the similar profile OL curves (Fig. 2(h)) of water up to 8 mJ cm^{-2}. However, on a further increase of laser fluence lead to multi-photon absorption, which could eventually lead to a decrease in the output laser fluence, which showing the OL behavior. Fig. 3(a–d) shows the SEM images and size distribution of W, Sn, Zn and In NPs, whereas Fig. 3(e) indicates the UV absorption spectra. The SPR peaks for these NPs are located near to 322, 245, 236, and 252 nm, respectively. Among all, Sn NPs have smallest size distribution lied between 3 and 12 nm, having a mean size at 8 nm.

Fig. 3(f) shows the OL curves for W, Sn, Zn and In NPs prepared by laser ablation using ps pulses. Zn and In NPs shows different OL behavior (shows the influence of SA beyond the input fluence of 25 mJ cm^{-2}) as compared to W and Sn NPs. Consequently, Sn NPs show higher optical nonlinearity as compared to that of W, Zn, and In NPs suspensions, due to their small particle size (~6 nm). The W and Sn NPs have a lower limiting threshold than the W and Sn (see Table .1).

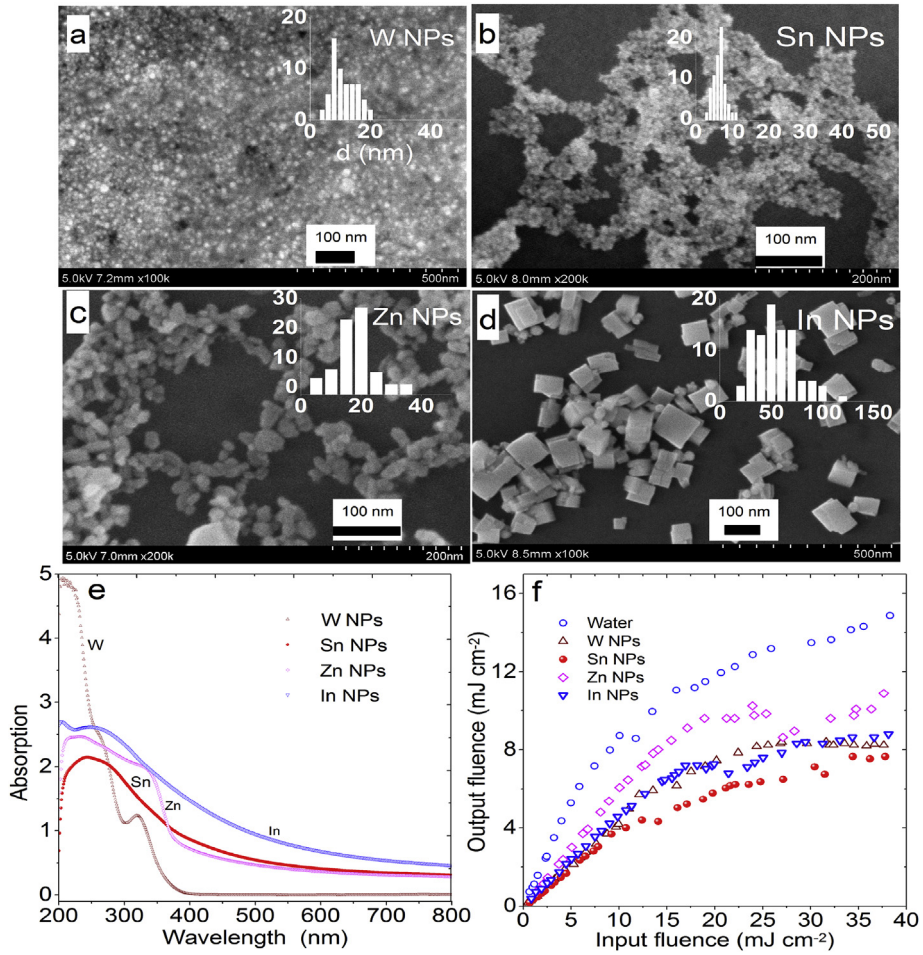

Fig. 3. SEM images and size distribution of (a) W NPs, (b) Sn NPs, (c) Zn NPs, (d) In NPs. (e) UV absorption spectra, and (f) optical limiting curves for Zn, Sn, In, and W NPs suspensions.

3.2. Characterization and optical limiting in Ni, Ti and Co nanoparticle suspensions

Fig. 4(d) demonstrates the UV-visible absorption spectra of Ti and Co NPs ablated in water. The Ti NPs have characteristic absorption surface plasmon resonance (SPR) peak at ~280 nm. Ti NP suspension initiates to absorb at ~500 nm. Previously, Barmina et al. reported that Ti NPs have an absorption peak at 530 nm while ablating by 355 nm, 150 ps pulses in water [30]. It was shown earlier that the Ti NPs change their SPR in the case of different composites of materials [31,32]. The synthesis of pure titanium nanoparticles in liquid by laser ablation method is not a simple task, because titanium is an active material. For the preparation of pure titanium NPs one has to add a surfactant, such as a polyvinylpyrrolidone which prevents the aggregation of titanium nanoparticle with oxide in water solution. The self-aggregation process of TiO depends on the type of liquid in which ablation carried out. In the case of ablation of Ti target in dichloroethane, the formation of TiC was demonstrated in Ref. [33]. In our case, we used fresh ablated suspension for study the optical limiting effect in pure Ti NPs. We also carried out the measurements of the nonlinear optical parameters of Ti NPs using Z-scan technique [34]. We used the suspension prepared just after laser ablation of pure Ti target in water. The LSPR for pure Ti NPs was observed at the wavelength of 280 nm.

The Co NPs in water shows some absorption peaks at 400 nm and 700 nm, respectively. Earlier studies demonstrated that some contradicting results on the position of SPRs of Co NPs, which probably can be attributed to different methods of NP formation and different spatial shapes of these small-sized species [35,36]. The absorption spectra of Ni NPS shows strong absorption near to 200 nm with the beginning of the broad absorption bands around 400 nm. Earlier, several efforts have been made for explanation of the appearance of the absorption band at 400 nm, which as assigned to the SPR in Ni NPs [37,38]. It has been explicitly shown the presence of two absorption bands in Ni NPs absorption spectra centered at 345 nm and 217 nm which were assigned to the SPR of Ni and interband d–d transition in Ni, respectively. Fig. 4(a–c) shows the SEM images and size distributions of the Ni, Ti, and Co NPs, the corresponding size distribution of lied between 30–200, 30–250, and 50–200 nm range at the mean size of 75, 125 and 90 nm, respectively.

Fig. 4(e) shows the results of OL properties of Ni, Ti and Co NPs. Ti and Co NPs in water shows high OL limiting properties compared to Ni NPs. The transmittance of Ni NPs suspension remained unchanged up to the input fluence of 10 mJ cm^{-2}. Then the transmittance decreased upon the increase of input fluence above OL threshold. This observation led to a conclusion that, at the higher input fluence or intensity, the NPs suspension exhibits 2 PA. Similar to the Ni NPs, Co NPs possess 2 PA, whereas Ti NPs show SA in deionized water at a lower fluence of 800 nm pulses. However, the Ti NPs show comparatively higher OL property compared to Ni NPs and similar response with the Co NPs. The OL thresholds for Ni, Ti and Co NPs in water are 10, 7.6 and 8 mJ cm^{-2} respectively. Ti and Co NPs in water show higher nonlinearity compared to Ni NPs.

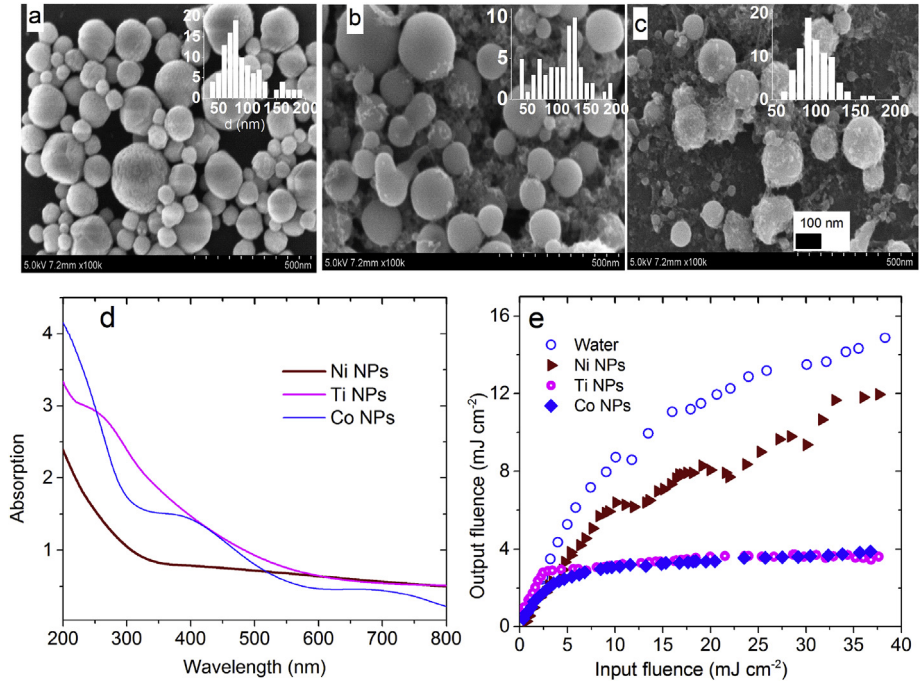

Fig. 4. SEM images and size distribution of (a) Ni NPs, (b) Ti NPs, (c) Co NPs. (d) UV absorption spectra, (e) optical limiting curves for these NPs suspensions.

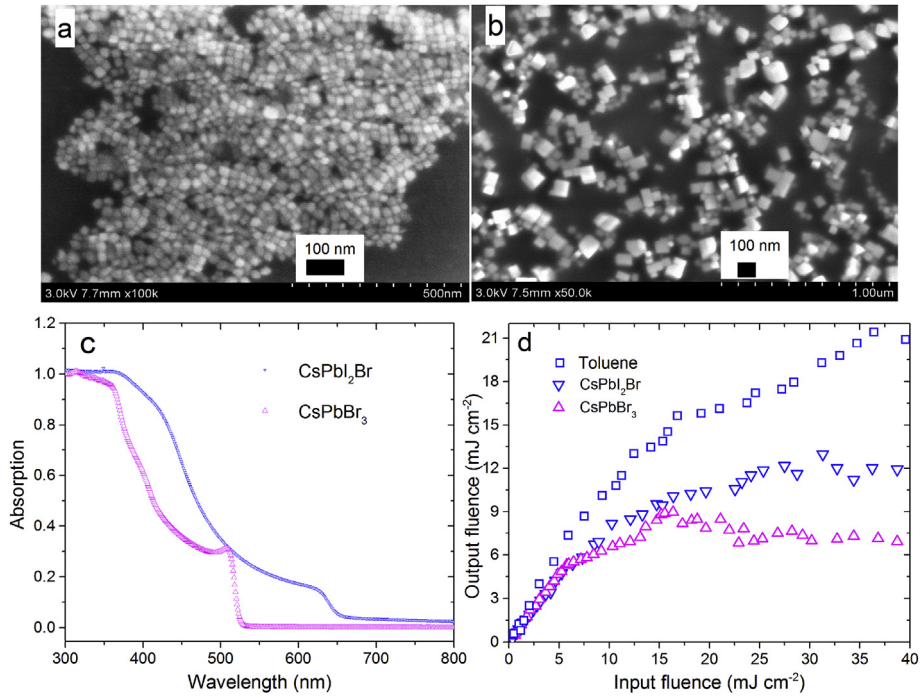

Fig. 5. SEM images of (a) $CsPbI_2Br$ (b) $CsPbBr_3$. (c) UV absorption spectra, and (d) optical limiting in $CsPbBr_3$ (upper open triangles) and $CsPbI_2Br$ (lower open triangles) perovskites and pure toluene (open squares).

3.3. Characterization and optical limiting in $CsPbBr_3$, and $CsPbI_2Br$ perovskite nanocrystals

Fig. 5(a and b) shows the SEM images, Fig. 5(c) show the UV-visible absorption spectra of $CsPbI_2Br$ and $CsPbBr_3$ perovskite nanocrystals. The rise in the absorption initiated in the case of $CsPbI_2Br$ and $CsPbBr_3$ is 650 nm and 530 nm, respectively. These perovskite nanocrystals possess the cubic shape, $CsPbI_2Br$ having the smaller size compared to $CsPbBr_3$ is shown in Fig. 5(a and b). The OL behavior of perovskites nanocrystals is high compared to the pure toluene (Fig. 5d, open triangles). However, QDs (Ag_2S QDs, Fig. 2(h)) having higher OL property compared to perovskite nanocrystals (Fig. 5(d)). The OL_T of Ag_2S QDs is 10.2 mJ cm^{-2}. $CsPbI_2Br$ and $CsPbBr_3$ perovskites have 6.2 and 13.2 mJ cm^{-2} thresholds, respectively. It was observed that under higher laser fluence $CsPbBr_3$ has the highest value of OL_T, even though it has higher volume of nanocrystal. OL in the case of $CsPbI_2Br$ shows conventional behavior compared to $CsPbBr_3$. Up to laser fluence of 12.5 mJ cm^{-2} the OL curve of $CsPbBr_3$ is similar to $CsPbI_2Br$. Beyond the laser fluence 12.5 mJ cm^{-2}, the effect of saturation of 2 PA was observed in case of $CsPbBr_3$. However, under high laser fluence $CsPbBr_3$

shows high OL behavior. The 2 PA in metal NPs, Ag_2S QDs and perovskites is known to be accompanied by the formation of free carriers, which also contribute to the nonlinear character of light propagation in these media. The interaction of the propagating radiation with these newly formed charge carriers can result in self-defocusing. One should distinguish the third-order nonlinearities caused by cumulative processes of absorption and free carrier generation from those caused by electronic processes.

The perfect OL materials should have a high transmission for low energies of radiation and limited transmission for higher energies. Since the optical limiters are based mainly on two effects, 2 PA and RSA, the real conditions of their application become the determining factor. The 2 PA is a function of the radiation intensity, while the RSA depends on the energy density of radiation. Thus, if one needs to limit the femtosecond, as well as the picosecond, radiation, the 2 PA is preferable and, conversely, materials exhibiting the RSA will be more efficient if one needs to limit longer pulses i.e. nanosecond to microsecond radiation [39].

4. Conclusions

The comparative study of absorptive optical limiting properties of Al, Ti, Co, Ni, Zn, Ag, Sn, In, W, Au NPs and Ag_2S quantum dots as well as $CsPbBr_3$ and $CsPbI_2Br$ perovskites carried out by 800 nm pulses of duration 60 fs has been reported. It was observed that the nanoparticles with small sizes possess the strong optical limiting properties comparatively. The magnetic NPs and perovskites nanocrystals show comparatively higher nonlinear absorption coefficients, which can also be used for optical limiting. Among the reported NPs, QDs and perovskites, Au NPs, Sn NPs, Ag_2S QDs, and $CsPbBr_3$ show the higher optical limiting properties.

Acknowledgments

The financial support from National Key Research and Development Program of China (2017YFB110470), National Natural Science Foundation of China (NSFC, 91750205, 61774155, 61705227), and Jilin Science and Technology Department Project (20150204019GX) is appreciated. R.A.G. acknowledges the financial support from the Chinese Academy of Sciences President's International Fellowship Initiative (Grant No. 2018VSA0001).

References

[1] S. Qu, C. Du, Y. Song, Y. Wang, Y. Gao, Optical nonlinearities and optical limiting properties in gold nanoparticles protected by ligands, Chem. Phys. Lett. 356 (2002) 403–408 https://doi.org/10.1016/S0009-2614(02)00396-2.
[2] Y. Gao, Q. Chang, H. Ye, W. Jiao, Y. Li, Y. Wang, Y. Song, D. Zhu, Size effect of optical limiting in gold nanoparticles, Chem. Phys. 336 (2007) 99–102, https://doi.org/10.1016/j.chemphys.2007.05.011.
[3] J. Gangareddy, E. Bheemaiah, V. Gandhiraj, J.T. James, J.K. Jose, K. Katturi Naga, S. Venugopal Rao, Nonlinear optical studies of sodium borate glasses embedded with gold nanoparticles, Appl. Phys. B 124 (2018) 205, https://doi.org/10.1007/s00340-018-7074-y.
[4] M. Anija, J. Thomas, N. Singh, A.S. Nair, R.T. Tom, T. Pradeep, R. Philip, Nonlinear light transmission through oxide-protected Au and Ag nanoparticles : an investigation in the nanosecond domain, Chem. Phys. Lett. 380 (2003) 223–229, https://doi.org/10.1016/j.cplett.2003.09.023.
[5] R. Philip, G.R. Kumar, Picosecond optical nonlinearity in monolayer-protected gold , silver , and gold-silver alloy nanoclusters, Phys. Rev. B 62 (2000) 160–166 DOI:10.1103PhysRevB.62.13160.
[6] S. Cai, X. Xiao, X. Ye, W. Li, C. Zheng, Nonlinear optical and optical limiting properties of ultra-long gold nanowires, Mater. Lett. 166 (2016) 51–54 https://doi.org/10.1016/j.matlet.2015.12.039.
[7] R. Gomathi, S. Madeswaran, D.R. Babu, G. Aravindan, Nonlinear optical, optical limiting and dielectric properties of organic cyclohexylammonium acetate single crystal, Mater. Lett. 209 (2017) 240–243 https://doi.org/10.1016/j.matlet.2017.08.016.
[8] C. Zheng, W. Chen, H. Wang, W. Li, Synthesis of copper oxide dots assembly on copper silicate nanorods and their optical limiting properties, Mater. Lett. 198 (2017) 42–45 https://doi.org/10.1016/j.matlet.2017.03.120.
[9] P. Pradhan, R. Podila, M. Molli, A. Kaniyoor, V.S. Muthukumar, S.S. Sankara, S. Ramaprabhu, A.M. Rao, Optical limiting and nonlinear optical properties of gold-decorated graphene nanocomposites, Opt. Mater. (Amst). 39 (2015) 182–187, https://doi.org/10.1016/j.optmat.2014.11.023.
[10] X.-L. Zhang, X. Zhao, Z.-B. Liu, Y.-S. Liu, Y.-S. Chen, J.-G. Tian, Enhanced nonlinear optical properties of graphene-oligothiophene hybrid material, Optic Express 17 (2009) 23959–23964, https://doi.org/10.1364/OE.17.023959.
[11] Q. Ouyang, X. Di, Z. Lei, L. Qi, C. Li, Y. Chen, Enhanced reverse saturable absorption in graphene/Ag2S organic glasses, Phys. Chem. Chem. Phys. 15 (2013) 11048–11053, https://doi.org/10.1039/C3CP51154E.
[12] L.W. Tutt, T.F. Boggess, A review of optical limiting mechanisms and devices using organics, fullerenes, semiconductors and other materials, Prog. Quant. Electron. 17 (1993) 299–338 https://doi.org/10.1016/0079-6727(93)90004-S.
[13] R. Kuladeep, L. Jyothi, P. Prakash, S.M. Shekhar, M.D. Prasad, D.N. Rao, Pulsed laser ablation in different carrier media Investigation of optical limiting properties of Aluminium nanoparticles prepared by pulsed laser ablation in different carrier media, J. Appl. Phys. 114 (2013) 243101, https://doi.org/10.1063/1.4852976.
[14] K. Zhang, R.A. Ganeev, G.S. Boltaev, P.V. Redkin, C. Guo, Effect of different hardness and melting point of the metallic surfaces on structural and optical properties of synthesized nanoparticles, Mater. Res. Express 6 (2019) 045027, , https://doi.org/10.1088/2053-1591/aafc0d.
[15] G.S. Boltaev, R.A. Ganeev, P.S. Krishnendu, S.K. Maurya, P.V. Redkin, K.S. Rao, K. Zhang, C. Guo, Strong third-order optical nonlinearities of Ag nanoparticles synthesized by laser ablation of bulk silver in water and air, Appl. Phys. A 124 (2018) 766, https://doi.org/10.1007/s00339-018-2195-z.
[16] L.W. Tutt, A. Kost, Optical limiting performance of C60 and C70 solutions, Nature 356 (1992) 225–226, https://doi.org/10.1038/356225a0.
[17] L. Wang, Q. Li, H. Wang, J. Huang, R. Zhang, Q. Chen, H. Xu, W. Han, Z. Shao, H. Sun, Ultrafast optical spectroscopy of surface-modified silicon quantum dots : unraveling the underlying mechanism of the ultrabright and color-tunable photoluminescence, Light Sci. Appl. 4 (2015) 1–8, https://doi.org/10.1038/lsa.2015.18.
[18] S.L. Diedenhofen, D. Kufer, T. Lasanta, G. Konstantatos, Integrated colloidal quantum dot photodetectors with color-tunable plasmonic nanofocusing lenses, Light Sci. Appl. 4 (2015) 1–7, https://doi.org/10.1038/lsa.2015.7.
[19] J.J. Joos, L.I.D.J. Martin, Z. Hens, P.F. Smet, Hybrid remote quantum dot/powder phosphor designs for display backlights, Light Sci. Appl. 6 (2017) 1–9, https://doi.org/10.1038/lsa.2016.271.
[20] L. Gu, Z. Fan, Perovskite/organic-semiconductor heterojunctions for ultrasensitive photodetection, Light Sci. Appl. 6 (2017) e17090, , https://doi.org/10.1038/lsa.2017.90.
[21] S.P.P. Sadhu, P.W. Jaschin, S. Perumbilavil, A.R. Thomas, V. Sai Muthukumar, R. Philip, K.B.R. Varma, Nonlinear optical properties of lead-free ferroelectric nanostructured perovskite, Appl. Phys. B 124 (2018) 200, https://doi.org/10.1007/s00340-018-7062-2.
[22] G.S. He, S.H. Liu, Physics of Nonlinear Optics, World scientific publishing, 1999.
[23] M. Rashidian, D. Dorranian, Investigation of optical limiting in nanometals, Rev. Adv. Mater. Sci. 40 (2015) 110–126.
[24] G.S. Boltaev, D.J. Fu, B.R. Sobirov, M.S. Smirnov, O. Vchinnikov, A.I. Zvyagin, R.A. Ganeev, Optical limiting , nonlinear refraction and nonlinear absorption of the associates of Cd 0 . 5 Zn 0 . 5 S quantum dots and dyes, Optic Express 26 (2018) 13865–13875 https://doi.org/10.1364/OE.26.013865.
[25] L. Sutherland, Handbook of Nonlinear Optics, Marcel Dekker, New York, 2003.
[26] U. Gurudas, E. Brooks, D.M. Bubb, S. Heiroth, T. Lippert, A. Wokaun, M. Group, P.S. Institut, C.-V. Psi, Saturable and reverse saturable absorption in silver nanodots at 532 nm using picosecond laser pulses, J. Appl. Phys. 104 (2008) 1–8, https://doi.org/10.1063/1.2990056 073107.
[27] C. Zheng, J. Huang, L. Lei, W. Chen, H. Wang, W. Li, Nanosecond nonlinear optical and optical limiting properties of hollow gold nanocages, Appl. Phys. B 124 (2017) 17, https://doi.org/10.1007/s00340-017-6888-3.
[28] Y.-P. Sun, J.E. Riggs, H.W. Rollins, R. Guduru, Strong optical limiting of silver-containing nanocrystalline particles in stable suspensions, J. Phys. Chem. B 103 (1999) 77–82, https://doi.org/10.1021/jp9835014.
[29] M. Hari, S. Mathew, B. Nithyaja, S.A. Joseph, V.P.N. Nampoori, P. Radhakrishnan, Saturable and reverse saturable absorption in aqueous silver nanoparticles at off-resonant wavelength, Opt. Quant. Electron. 43 (2012) 49–58, https://doi.org/10.1007/s11082-011-9502-7.
[30] E.B. Barmina, E. Stratakis, C. Fotakis, G.A. Shafeev, Generation of nanostructures on metals by laser ablation in liquids : new results Generation of nanostructures on metals by laser ablation in liquids : new results, Quant. Electron. 40 (2010) 1012–1020, https://doi.org/10.1070/QE2010v040n11ABEH014444.
[31] M. Torrell, R.C. Adochite, L. Cunha, N.P. Barradas, E. Alves, M.F. Beaufort, J.P. Rivière, A. Cavaleiro, S. Dosta, F. Vaz, Surface plasmon resonance effect on the optical properties of TiO 2 doped by noble metals nanoparticles, J. Nano Res. 19 (2012) 177–185, https://doi.org/10.4028/www.scientific.net/JNanoR.18-19.177.
[32] J.Z. Hang, T.P.C. Hen, Y.C.L. Iu, Y.L. Iu, H.Y.Y. Ang, Investigation of localized surface plasmon resonance of TiN nanoparticles in TiN x O y thin films, Opt. Mater. Express 6 (2016) 285–291.
[33] S.I. Dolgaev, A. V Simakin, V. V Voronov, G.A. Shafeev, F. Bozon-verduraz, Nanoparticles produced by laser ablation of solids in liquid environment, Appl. Surf. Sci. 186 (2002) 546–551.
[34] K.S. Rao, R.A. Ganeev, K. Zhang, Y. Fu, G.S. Boltaev, P. Krishnendu, P.V. Redkin, C. Guo, Laser ablation – induced synthesis and nonlinear optical characterization of titanium and cobalt nanoparticles, J. Nanoparticle Res. 20 (2018) 285 2018.
[35] G. Simon, L. Meziane, A. Courty, I. Lisiecki, Low wavenumber Raman scattering of cobalt nanoparticles self-organized in 3D superlattices far from surface plasmon resonance, J. Raman Spectrosc. 47 (2016) 248–251, https://doi.org/10.1002/jrs.4782.

[36] D.A. Yashunin, A.I. Korytin, Localized Plasmon resonance in metal nanoparticles using Mie theory Localized Plasmon resonance in metal nanoparticles using Mie theory, J. Phys. Conf. Ser. 850 (2017) 012017, , https://doi.org/10.1088/1742-6596/850/1/012017.

[37] H. Amekura, H. Kitazawa, N. Umeda, Y. Takeda, N. Kishimoto, Nickel nanoparticles in silica glass fabricated by 60 keV negative-ion implantation, Nucl. Instrum. Methods Phys. Res. Sect. B Beam Interact. Mater. Atoms 222 (2004) 114–122 https://doi.org/10.1016/j.nimb.2004.01.214.

[38] T. Isobe, S.Y. Park, R.A. Weeks, R.A. Zuhr, The optical and magnetic properties of Ni + -implanted silica, J. Non-Cryst. Solids 189 (1995) 173–180 https://doi.org/10.1016/0022-3093(95)00230-8.

[39] R.A. Ganeev, A.I. Ryasnyanski, M.K. Kodirov, Optical limiting in fullerenes , colloidal metal solutions , and semiconductors in the field of pico- and nanosecond pulses of an Nd : YAG laser, Optic Spectrosc. 93 (2002) 789–796, https://doi.org/10.1134/1.1524003.